POLITECNICO
MILANO 1863

SCUOLA DI INGEGNERIA INDUSTRIALE
E DELL'INFORMAZIONE

Executive Summary of the Thesis

Scaling Relations for the Geometry of Wire to Airfoil Atmospheric Ionic Thrusters

Laurea Magistrale in Aeronautical Engineering - Ingegneria Aeronautica

Author: Omar Kahol

Advisor: Prof. Marco Belan

Academic year: 2022-2023

1. Introduction

In recent years, the aerospace industry has undergone a significant shift towards sustainability and efficiency, with a strong emphasis on reducing the environmental impact of its operations. As a result, there is now a concerted effort to explore green alternatives to traditional fossil fuel propulsion systems. One such alternative that has gained considerable traction in the industry is electric propulsion, with electrohydrodynamic (EHD) propulsion emerging as a particularly promising technology. While EHD thrusters have long been used in space applications, they are now increasingly being viewed as a viable option for atmospheric flight as well. This is largely due to the fact that EHD propulsion offers a range of benefits, including an exceptional thrust to power ratio, a lack of moving parts, and low noise emissions.

In its simplest form, a conventional EHD thruster comprises of two electrodes that are subjected to a high voltage difference. The first electrode, known as the emitter, is typically a wire with a very small curvature radius, usually below 100 µm. When a high voltage is applied to the emitter, it creates a strong electric field that ionizes the surrounding air, resulting in the formation of the Corona Discharge. The second electrode, which is located at a distance referred to as the gap, d, from the emitter, is usually a large aerodynamic shape designed in such a way that ionization does not occur. This arrangement creates a strong asymmetric electric field that attracts the ions towards it. The ions are then accelerated by the electric field and exchange their kinetic energy with the neutral gas, leading to the creation of an airflow and a propelling force.

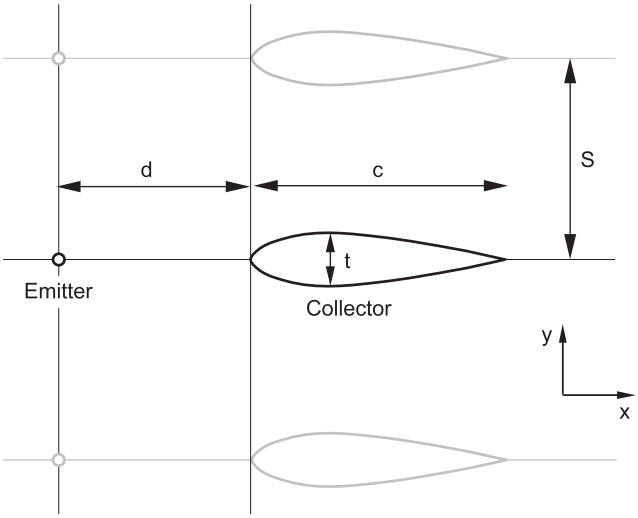

Figure 1: Geometrical parameters of EHD thrusters.

A possible way to arrange multiple thrust generating cells is depicted in Figure 1. In this case, multiple cells, consisting of a single emitter and a single NACA collector of chord c and thickness t, are stacked together at a spacing S.
In 2018 a research team from MIT [8] successfully powered a small airplane in level flight with power supply on board. Khomich et al. [6, 7] built a lifter with outboard power supply, proving that optimized EHD configurations can produce a lifting force greater than the weight of the system. Ieta et al. [3–5] used corona discharge to power a small propeller.
These works, along with many others, study different geometries and the effect of different parameters. Current state of the art literature, however, lacks a proper multi-parametric investigation and evaluation of the possible geometrical parameters as well as a framework in which performance parameters should be evaluated. As far the geometry is concerned, the effect of the chord of the collector has not been studied and many authors use either cylinders or NACA0010 airfoils with a chord of 100 mm.
For these reasons, this work is focused on the development of a dimensionless scaling model that extracts from the governing equations physically consistent reference values and dimensionless coefficients. This work also explores the functional form of these dimensionless coefficients by means of an extensive and complete experimental investigation.

2. Dimensionless Model

The dimensionless model is applied to the drift region equations which are the equations that govern the motion of ionized species in the drift region. These equations are Maxwell's law of electric fields, the conservation of current and the conservation of momentum for the neutral gas

$$\begin{cases} \nabla \cdot \mathbf{E} = \rho_q/\epsilon_0 \\ \nabla \cdot \rho_q \left(\mu_q \mathbf{E} + \mathbf{u}\right) = 0 \\ \rho \mathbf{u} \cdot \nabla \mathbf{u} = -\nabla P + \mu \nabla^2 \mathbf{u} + \rho_q \mathbf{E} \end{cases} \tag{1}$$

The equations are made dimensionless using the gap, d, as a reference length and the applied voltage to gap ratio V_a/d as the reference electric field. This process helps to extract reference values and dimensionless coefficients for each performance parameter

$$\text{Thrust, } \mathrm{T} = \epsilon_0 \frac{\mathrm{V_a^2}}{\mathrm{d}}\ \mathrm{C_T}\ , \tag{2}$$

$$\text{Power, } \mathrm{P} = \mu_\mathrm{q} \epsilon_0 \frac{\mathrm{V_a^3}}{\mathrm{d^2}}\ \mathrm{C_P}\ , \tag{3}$$

$$\text{Thrust to Power, } \mathrm{T/P} = \frac{\mathrm{d}}{\mathrm{V_a}\mu_\mathrm{q}}\ \mathrm{C_{TP}}\ , \tag{4}$$

$$\text{Thrust Density, } \mathrm{T/A} = \epsilon_0 \frac{\mathrm{V_a^2}}{\mathrm{d^2}}\ \mathrm{C_{TA}}\ . \tag{5}$$

The reference values show how the performance indicators scale as the gap and applied voltage change whereas the dimensionless coefficients (all of order one) are a function of the dimensionless variables. In particular, the dimensionless variables explored in this work are $t/d,\ c/d,\ S/d,\ V_a/V_i$.

3. Experimental Setup

In this study, load measurements are performed using an experimental setup that employs load cells to directly measure the thrust.

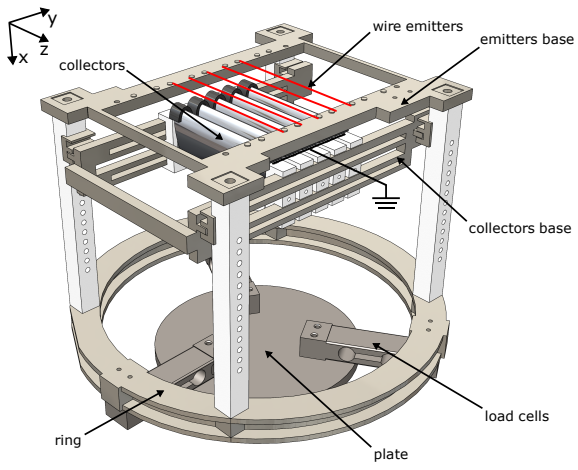

Figure 2: Load Measurement experimental setup.

The main components of the test rig, made of insulating materials with 3D printing, include the anode base, the collector base, and the ring, as shown in detail in Figure 2. Five airfoil-shaped collectors are tested to create an array that approximates periodic conditions on the outflow near the central collector. Anodes consist of a constantan wire with a diameter of 30 μm that

is tensed above the collectors in the spanwise direction. The test rig allows for discrete variations of the inter-collector spacing, inter-emitter spacing, and inter-electrodes gap, necessary to perform different parametric analyses. The system is powered by a power supply capable of up to 6 mA and a voltage range of 0 V to +20 kV; the collectors are grounded by means of a thin aluminum conductive strip on the airfoil surface and connected to the main ground via thin cables. An oscilloscope is used to acquire all output signals to obtain electrical and thrust measurements.

Three identical load cells, capable of a full scale of 7.5 N and a precision of ±1 mN, are arranged in a radial configuration to perform the load measurements. They support the weight of the entire structure of the ionic thruster. When high voltage is applied to the system, the net force exerted by the ionic wind reduces the load applied to the cells, which can be used to retrieve the net thrust generated by the thruster. A simple procedure is used to convert the voltage signals coming from the load cells through a signal conditioner. An accurate procedure with multiple measures was used to reduce casual and systematic errors, resulting in uncertainties in the thrust order of ±1 mN. In addition to load measurements, electrical measurements are performed during the tests, including the voltage between the electrodes V_c and the current flowing in the circuit I_{tot}, which are continuously measured. The power supply current consumption I_{tot} is measured by means of the ammeter integrated in the power supply unit, with an accuracy of ±0.01 mA, resulting in an uncertainty on the power consumption of ±0.1 W. A shunt resistor is added to ground the collectors and measure the corona current i_c. It is used to perform electrical measurements for troubleshooting leakages and for the acquisition of the corona inception voltage, an important quantity related to the ionization region of corona discharge that is experimentally measured for every configuration to estimate the real applied voltage necessary for the corona discharge to ignite in the tested ionic thruster. This is used as an electrical performance parameter to characterize the phenomenon from an electrical point of view. The uncertainties of this measurement due to systematic errors were estimated to be ±200 V.

4. Research Parameters

The main goal of this work is the exploration of the functional dependence of the performance coefficients on the dimensionless parameters. Also, it was important to demonstrate that thin airfoils with a small chord are capable of optimizing the performances. For this reason, a total of 13 airfoils of different chord and thickness were studied.

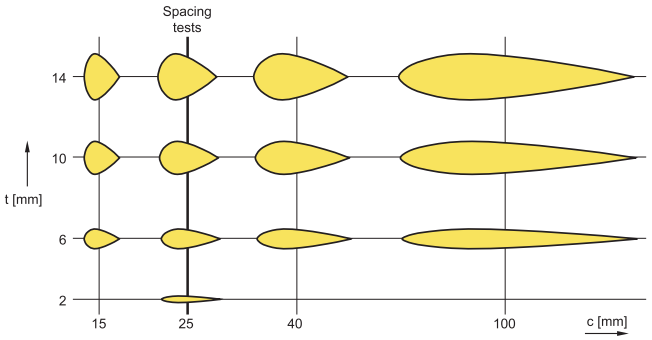

Figure 3: Depiction of the different airfoils that were studied in this thesis.

Figure 3 depicts the various airfoils that were evaluated in this study. The objective was to build upon the findings of Belan et al.[2], who demonstrated that, if the chord is 100 mm, the NACA0010 airfoil provides optimal performance across all indicators. To reduce aerodynamic drag while keeping electrical thrust constant, the chord length was gradually decreased while maintaining constant thickness. However, this approach was limited by the occurrence of flow separation when the airfoils became excessively bluff.

In addition, inter-collector spacing was investigated by varying the distance between the collectors from the minimum possible value for the given airfoil thickness to 35 mm, which approximates the spacing in isolated cells. The gap between the collectors was also adjusted within the range of 10 mm to 30 mm. Since the gap is chosen as a reference length, its variation will cause variations in S/d, c/d, and t/d combined.

5. Results

This section is dedicated to the presentation of the main results.

5.1. Chord and Thickness dependence

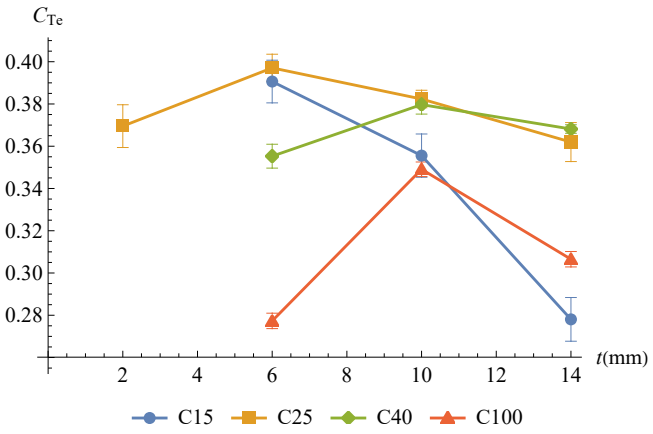

Figure 4: Thrust Coefficient

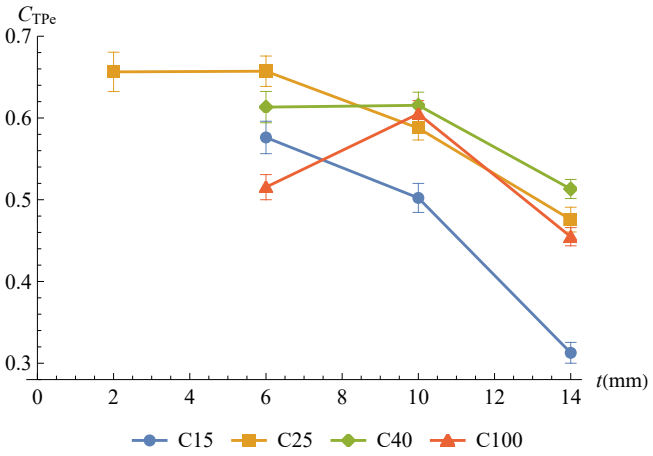

Figure 5: Thrust to Power Coefficient

Figures 4 and 5 show the behaviour of the thrust and thrust to power coefficient as a function of the airfoil thickness and for different airfoil chords. The evaluation is performed at a gap of 20 mm, a spacing of 35 mm and an applied voltage of 20 kV. These graphs show that a reduction of the chord is beneficial as the airfoil develops less parasitic drag. This must, however, be accompanied by a reduction of the thickness in order to reduce the t/c parameter, which is linked to flow separation, and the S/t parameter which controls the blockage effects caused by nearby collectors. Decreasing the chord also increases the power consumption coefficient and therefore, while the thrust could theoretically be further increased, the thrust to power reaches a maximum value for the C25T6 configuration.

5.2. Spacing dependence

The spacing between the units was also decreased, keeping the applied voltage fixed, in order to increase the thrust density by reducing the frontal area of the thruster.

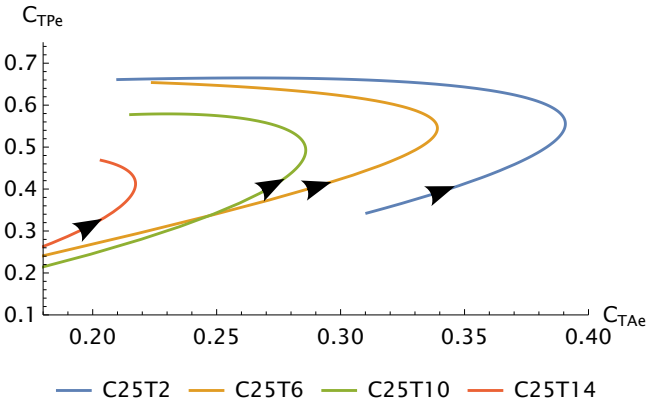

Figure 6: C_{TA}-C_{TP} curves for the C25 airfoil family. The arrows indicate directions of increasing spacing.

Figure 6 shows that decreasing the spacing is beneficial for the thrust density because the reduction is thrust is compensated by a reduction in the frontal area. A local optimum can be found because at low enough spacing the generated thrust decreases exponentially and is not able to compensate the decreases of the frontal area. The curves exhibit a local Pareto frontier which occurs for the C25T2 airfoil. The same configuration was also tested in a double emitter configuration, which was initially proposed by Belan et al.[1], indicating that the latter can improve the thrust to power of large spacing configurations.

5.3. Gap and Voltage dependence

The gap and applied voltage parameters were also varied to investigate their effect on the performance parameters. The results indicate excellent agreement with the scaling model introduced in Section 2; in particular, decreasing the gap increases both the generated thrust and the power consumption. The thrust to power of the unit, however, decreases as the gap is decreased. This is due to the fact that the power increases quadratically while the thrust linearly.

The voltage dependence is well predicted by a 1D model.

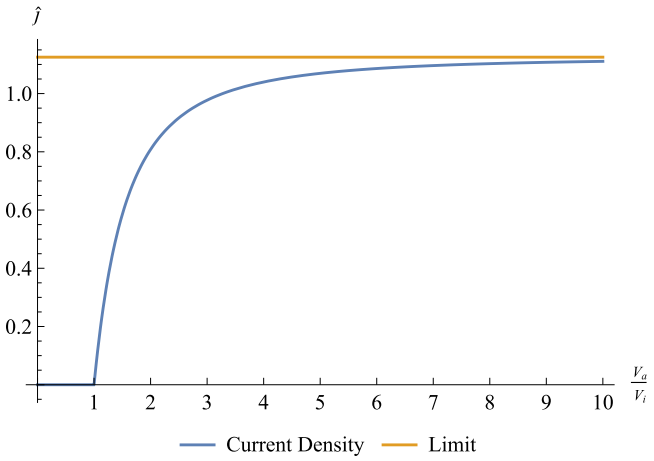

Figure 7: Current density coefficient dependence on the dimensionless voltage.

Figure 7 shows that the current density coefficient, which in 1D is equal to the thrust and power coefficient, exhibits a linear behaviour in the region where the applied voltage is close to the inception voltage (which is the minimum voltage required for corona inception). At relatively high voltages applied voltages (4/5 times the inception voltage), the dimensionless coefficients approach a constant value.

6. Conclusions

The main result of this study is the development of a dimensionless model which helped to define physically consistent reference values, dimensionless coefficients and dimensionless variables. A theoretical prediction of the functional form of the dimensionless coefficient is, however, possible only under strong simplifying assumptions such as 1D configurations. Nevertheless, this study provides a global framework in which the performance and behaviour of different configurations can be analyzed. Moreover, an extensive experimental campaigned allowed to study the effect of different geometrical dimensionless parameters on the performance indicators. The results, apart from showing interesting and global trends, indicate that a reduction of the airfoil chord is beneficial for the efficiency of the thruster and that optimal configurations can be found within the proposed experimental parameter space.

References

[1] M. Belan, R. Terenzi, S. Trovato, and D. Usuelli. Effects of the emitters density on the performance of an atmospheric ionic thruster. *Journal of Electrostatics*, 120:103767, 2022.

[2] Marco Belan, Luca Arosti, Riccardo Polatti, Filippo Maggi, Samuele Fiorini, and Federico Sottovia. A parametric study of electrodes geometries for atmospheric electrohydrodynamic propulsion. *Journal of Electrostatics*, 113:103616, 2021.

[3] M. Chirita and A. Ieta. First rotary ionic engine with contra-rotating propellers. *Journal of Propulsion and Power*, pages 1–8, 2022.

[4] A. Ieta and M. Chirita. Electrohydrodynamic propeller for in-atmosphere propulsion; rotational device first flight. *Journal of Electrostatics*, 2019.

[5] A. Ieta, R. Ellis, D.M. Citro, M. Chirita, and J. D'Antonio. Characterization of corona wind in a modular electrode configuration. 2013.

[6] V Yu Khomich and V A Yamshchikov. Electrohydrodynamic flow for the active control of gas flows. *Physics-Uspekhi*, 2017.

[7] V.Yu. Khomich and I.E. Rebrov. In-atmosphere electrohydrodynamic propulsion aircraft with wireless supply onboard. *Journal of Electrostatics*, 2018.

[8] H. Xu, Y. He, K. Strobel, C. Gilmore, S. Kelley, C. Hennick, T. Sebastian, M. Woolston, D. Perreault, and S.R.H. Barrett. Flight of an aeroplane with solid-state propulsion. *Nature*, 563, 11 2018.